Tomáš Březina
Ryszard Jabłoński
Editors

Mechatronics 2013

RECENT TECHNOLOGICAL AND SCIENTIFIC ADVANCES

Springer

Mechatronics 2013

Tomáš Březina · Ryszard Jabłoński
Editors

Mechatronics 2013

Recent Technological and Scientific Advances

Springer

Editors
Tomáš Březina
Faculty of Mechanical Engineering
Institute of Automation and Computer Science
Brno University of Technology
Brno
Czech Republic

Ryszard Jabłoński
Institute of Metrology and Biomedical Engineering
Warszaw University of Technology
Warszaw
Poland

ISBN 978-3-319-02293-2 ISBN 978-3-319-02294-9 (eBook)
DOI 10.1007/978-3-319-02294-9
Springer Cham Heidelberg New York Dordrecht London

Library of Congress Control Number: 2013947579

Printed on acid-free paper

Springer is part of Springer Science+Business Media (www.springer.com)

Preface

This book is the fourth volume in series Recent Advances in Mechatronics, following the editions in 2007, 2009 and 2011. It comprises carefully selected contributions presented at the 10th International Conference Mechatronics 2013, organized by Brno University of Technology on October 7–9, 2013 in Brno, Czech Republic.

The selection of the contributions for this book was based on thorough reviews of full length papers, concentrating on originality and quality of the work. Finally 113 papers were selected for publishing in this book.

The book covers the areas design, modeling and simulation of mechatronic systems, in particular the r&d of mechatronic systems, model-based design, virtual prototyping, electrical machines, drives & power electronics, actuators and sensors, automotive and aerospace systems, measurement and diagnostics, signal processing, pattern recognition, wireless sensing, nanometrology, industrial and mobile robotics, microrobotics, unmanned vehicles, control and automation, industrial applications, vibration and noise control, the list of topics could go on and on.

We hope that the volume can serve as useful reference source in mechatronics not just among academics, but also in development departments in industry, as the mechatronics as a subject should be closely related with the rapid transfer of new ideas to products we can meet in our daily lives.

We would like to thank all authors for their contribution to this book.

Tomáš Březina
Conference Chairman
Brno University of Technology

Contents

Design, Modeling and Simulation of Mechatronic Systems

Monitoring of Energy Flows in the Production Machines 1
J. Augste, M. Holub, R. Knoflíček, T. Novotný, J. Vyroubal

Off- Road Vehicle with Controlled Suspension in Soft Unprepared Terrain 9
A. Bílkovský, Z. Šika

The Manipulator of the Passive Optoelectronic Rangefinder as a Controlled System of Servomechanisms 17
V. Cech, M. Cervenka

Energy Management System Algorithms for the Electric Vehicle Applications 25
J. Danko, L. Magdolen, M. Masaryk, J. Madaras, M. Bugar

Virtual Commissioning of Mechatronic Systems with the Use of Simulation 33
J. Hloska, M. Kubín

Prediction of Machining Accuracy for Vertical Lathes 41
M. Holub, M. Michalíček, J. Vetiška, J. Marek

Towards to Haptic Keyboard: Modeling the Piano Action ... 49
P. Horváth

Gubanov Model for Vacuum Packed Particles 57
R. Zalewski, P. Chodkiewicz

Eco-design of Mechatronic Systems 65
M. Iskandirova, P. Blecha, M. Holub, F. Bradáč

Thick Film Polymer Composites with Graphene Nanoplatelets for Use in Printed Electronics 73
D. Janczak, M. Słoma, G. Wróblewski, A. Młożniak, M. Jakubowska

Safety Module for the System of Verticalization and Aiding Motion of the Disabled 79
D. Jasińska-Choromańska, B. Kabziński, M. Matyjewicz-Maciejewicz, D. Kołodziej

Electromagnetic Coil Gun – Construction and Basic Simulation 87
B. Skala, V. Kindl

Generating Code Consistent with Simulink Simulation for Aperiodic Execution on a Target Hardware Powered by a Free RTOS 95
V. Lamberský, J. Križan, A. Andreev

A New Approximation of the Storage Efficiency for the Lean NOx Trap Model 103
B. Lee, R. Grepl, M. Han

Overview of Computational Models Used for Mixed Lubrication 111
O. Maršálek, P. Novotný, P. Raffai, L. Drápal, V. Píštěk

Heating of Mould in Manufacture of Artificial Leathers in Automotive Industry 119
J. Mlynek, T. Martinec, R. Srb

Influence of Underpressure on Acoustic Properties of Semi-intelligent Vacuum Packed Particles 127
M. Rutkowski

Hardware in the Loop Simulation Model of BLDC Motor Taking Advantage of FPGA and CPU Simultaneous Implementation 135
V. Sova, R. Grepl

Using PSO Method for System Identification 143
M. Dub, A. Stefek

Damping of Machine Frame Vibrations by an Electromagnetic Actuator 151
G.J. Stein, R. Chmúrny

Determination of Parameters of Second Order Integration Model for Weighing Scales . . . 161
R. Ugodziński, R. Szewczyk

Feed-Rate Control along Multi-axis Toolpaths . . . 169
P. Vavruska

Model Based Design of Power HIL System for Aerospace Applications . . . 177
J. Vejlupek, J. Chalupa, R. Grepl

Visualization of Energy Flows Using a Particle System . . . 185
I. Dudarev, V. Wittstok, F. Pürzel, P. Blecha

Parameter Identification of Rheological Models Using Optimization Algorithms . . . 193
V. Píštěk, P. Novotný, T. Mauder, L. Klimeš

Cam Ring Force Simulation for Variable Roller Pump . . . 199
P. Zavadinka, R. Grepl

Benefits of a Parallelization of a Stand-Alone Desktop .NET Application Threaded Instance Methods . . . 207
I. Košťál

Morphing Structure with a Magnetorheological Material – Preliminary Approach . . . 219
P. Skalski

Evaluation of Possibilities of Electroactive Polymers Application in Bio-inspired Adaptronic System . . . 227
J. Kaleta, K. Kot, D. Lewandowski, K. Niemiec, P. Wiewiorski

Transport Duty Cycle Simulation of Electro-hydro-mechanical Drive Unit for Mixing Drum . . . 235
P. Kriššák, J. Jakubovič, P. Zavadinka

Investigation on the Jump Phenomenon of Linear Compressor . . . 243
H.M. Zou, M.S. Tang, Sh.Q. Shao, Ch.Q. Tian, Y.Y. Yan

Software Tool for Calibration of Hydraulic Models of Water-Supply Networks . . . 253
J. Kovar, J. Rucka

Practical Problems during Fuel Pump Development for Aerospace Industry . . . 259
P. Axman, R. Král, V. Axman, J. Berjak

Simulation Modelling of MEMS Thermoelectric Generators for Mechatronic Applications 265
L. Janak, Z. Ancik, Z. Hadas

Simulation Assessment of Suspension of Tool Vibrations during Machining 273
T. Březina, L. Březina, J. Marek, Z. Hadas, J. Vetiška

Electrical Machines, Drives and Power Electronics

The Comparison of the Permanent Magnet Position in Synchronous Machine 283
P. Svetlik

Air Gap Heat Transmission and Its Consideration in FEM Analyses 291
R. Pechanek, V. Kindl, K. Hruska

Problems of FEM Analysis of Magnetic Circuit 299
J. Roupec, M. Kubik, I. Mazůrek, Z. Strecker

FEM Model of Induction Machine's Air Gap Force Distribution 307
J. Sobra, V. Kindl

Current-Voltage Characteristics and IR Imaging of Organic Light-Emitting Diodes 315
G. Koziol, J. Gromek, A. Arazna, K. Janeczek, K. Futera, W. Steplewski

Complex Model of Asynchronous Machine as Traction Machine in Mining 323
R. Vlach

Energetic Properties of a New, Iron Powder Based Switched Reluctance Motor Drive 331
B. Fabianski

Switched Reluctance Motor Drive Embedded Control System 339
B. Fabianski, K. Zawirski

Design and Implementation of A Single-Stage Full-Bridge DC/DC Converter with ZVS Mode 347
A. Diker, D. Korkmaz, Ö.F. Alçin, U. Budak, M. Gedikpınar

Sensitivity Analysis of the Induction Machine Torque to the Substituting Circuit Elements 355
M. Patocka, R. Belousek

Fractional-Order Model of DC Motor 363
R. Cipin, C. Ondrusek, R. Huzlík

FEM Model of Electro-magnetic Vibration Energy Harvester 371
Z. Hadas, R. Huzlík

Measurement and Diagnostics

Contribution to Determination of Target Angular Position by Single Visual Camera at Indoor Close Environs 379
R. Doskocil, V. Krivanek, A. Stefek

A Simple Acoustic Generator for Boiler Cleaning Applications 387
A. Jedrusyna, A. Noga

Effects of Misalignments of MEMS Accelerometers in Tilt Measurements 393
S. Łuczak

Method for Determining Direction, Velocity and Position of a Flying Ball 401
A. Nagy

Silicon PIN Photodiode-Based Radiation Detector for Mobile Robots 409
O. Petruk, R. Szewczyk

A Method for Measuring Size and Form Deviations of Rotary Components with Variable Curvature on FMM 417
M. Sieniło, S. Żebrowska-Łucyk

Three-Dimensional Meshless Modelling of Functionally Graded Piezoelectric Sensor 425
P. Stanak, J. Sladek, V. Sladek, A. Tadeu

Diagnostics of Mechatronic Systems on the Basis of Neural Networks with High-Performance Data Collection 433
P. Stepanov, Yu. Nikitin

Signal Processing in DiaSter System for Simulation and Diagnostic Purposes 441
M. Syfert, P. Wnuk

System for Multipoint Measurements of Slowly Varying Magnetic Fields 449
M. Szumilas, E. Ślubowska, K. Lewenstein

X Band Power Generator 457
R. Krizan, L. Drazan

A New Approach to the Uncertainty in Diameter Measurement Using Laser Scanning Instrument 463
Ryszard Jablonski, Pawel Fotowicz

Real-Time Edge Detection Using Dynamic Structuring Element 471
M. Kawecki, B. Putz

Investigation Method for the Magnetoelastic Characteristics of Construction Steels in Nondestructive Testing 479
D. Jackiewicz, R. Szewczyk, J. Salach, A. Bieńkowski, K. Wolski

Testing of Automotive Park Assistant Control Unit by HIL Simulation 487
P. Krejci

Coupled Thermal-Structural Transient Analysis of Pressure Sensors 495
R. Vlach

Device for Measuring of Active Power and Energy at Machine Tools 503
R. Huzlík, P. Blecha, A. Vašíček, P. Houška, M. Holub

Robotics

Effect of Gear Ratio on Energy Consumption of Actuators Used in Orthotic Robot 511
K. Bagiński, J. Wierciak

Precise Model of Multicopter for Development of Algorithms for Autonomous Flight 519
R. Baranek, F. Solc

In-pipe Microrobot Driven by SMA Elements 527
M. Bodnicki, D. Kamiński

Adaptive Cruise Control for a Robotic Vehicle Using Fuzzy Logic 535
A. Hassan, G. Collier

Robot with Adjustable Undercarriage – The Design and the Simulation 543
M. Dovica, T. Kelemenová, M. Kelemen, T. Lukac

Project of Autonomous Control System in HUSAR Lunar Mining Rover 551
P. Węclewski, G. Bujko, P. Etz, Ł. Godziejewski, J. Kaplińska, P. Kicman, M. Wiśniowski

Object Classification Using Dempster–Shafer Theory 559
B. Harasymowicz-Boggio, B. Siemiątkowska

A Novel Indoor Localization Scheme by Integrating Wiimote Sensing and a Controllable IR-LED Array 567
Y.T. Fu, K.S. Chen

Hybrid Navigation Method for Dynamic Indoor Environment Based on Mixed Potential Fields 575
S. Vechet, K.S. Chen, J. Krejsa

Human-Machine Interface for Mobile Robot Based on Natural Language Processing 583
P. Mašek, M. Růžička

Real Time Object Tracking Based on Computer Vision 591
M. Růžička, P. Mašek

Searching for Features in Laser Rangefinder Scan via Combination of Local Curvature Scale and Human Obstacles Detection 599
J. Krejsa, S. Vechet

Orthotic Robot as a Self Optimizing System 607
J. Wierciak, K. Bagiński, D. Jasińska-Choromańska, T. Strojnowski

Trajectory Generation for Autonomous Vehicles 615
Vu Trieu Minh

Robotnic Underwater Vehicle Steered by a Gyroscope – Model of Navigation and Dynamics 627
E. Ładyżyńska-Kozdraś

Robotic Implementation of the Adaptive Cruise Control-Comparison of Three Control Methods 633
P. Shakouri, A. Ordys, G. Collier

Control and Automation

Self-learning Control for Servo Drives in Forming Technologies 641
M. Hoffmann, P. Hušek, H.-J. Koriath, V. Kučera, U. Priber

Automatic System for Object Recognition in Robotic Production Line for Automotive Industry 653
P. Božek, P. Pokorný

Pulse Response Identification of Inertial Model for Astatic System 663
J.E. Kurek

Benchmarking Various Rapid Control Prototyping Targets Supported in Matlab/Simulink Development Environment ... 669
V. Lamberský, R. Grepl

Tuning Rules Selection and Iterative Modification of PID Control System Parameters 677
J. Możaryn, K. Malinowski

Fuzzy Approach to the Selection of Interference Fit Assembly Method 685
A.N. Sinitsyn, V.V. Sinitsyna, I.V. Abramov, A.I. Abramov

Application of Artificial Neural Network for Speed Control of Servodrive with Variable Parameters 693
T. Pajchrowski

Hybrid Fuzzy – State Variable Feedback Controller of Inverted Pendulum 701
A. Petrovas, R. Rinkevičiene

A Model Comparison Performance Index for Servo Drive Control 709
J. Quellmalz, M. Rehm, H. Schlegel, W.-G. Drossel

Control Structures for Opposed Driving, Coupled Linear Drives 717
M. Rehm, J. Quellmalz, H. Schlegel, W.-G. Drossel

The Robust Remote Control of the Manipulator 725
V. Ondroušek, M. Vytečka, J. Kolomazník, M. Hammerschmiedt

Control System of One-Axis Vibration-Insulation Platform with Gyroscopic-Stabilizer 733
R. Votrubec

Hybrid PI Sliding Mode Position and Speed Controller for Direct Drive 741
S. Brock

Distributed Control System of Solar Domestic Hot Water Heating Using Open-Source 749
G. Gaspar, S. Pavlikova, R. Masarova

Design of Engine Control System for Small Helicopter 757
L. Ertl, M. Jasansky

Biomedical and Biomechanical Engineering

Application of Indices Characterizing the Shape of a Signal for Automatic Identification of Artifacts in Impedance Cardiography 763
P. Piskulak, G. Cybulski, W. Niewiadomski

Predictive Algorithm for the Insulin Dose Selection with Continuous Glucose Monitoring System 771
H.J. Hawłas, K. Lewenstein

Experimental Device for Reconstructing Spinal Deviations in to a 3D Model 779
F. Horvát, M. Čekan, L. Šoltés, B. Hučko

Automatic Analysis of Recurrence Plot for the Needs of the Analysis of Infrasonic Signals from the Human Heart 785
M. Jamrozy, K. Lewenstein, T. Leyko

Evaluation of the Empirical Mode Decomposition Method as a Tool for Preprocessing Ultrasonic Cardiological Data ... 793
T. Kubik, K. Kałużyński, S. Cygan, K. Mikołajczyk

Evaluation of Bilateral Asymmetry of the Muscular Forces Using OpenSim Software and Bilateral Cyclograms 801
P. Kutilek, Z. Svoboda, P. Smrcka

Properties of Ankle-Brachial-Index (ABI) in the Light of Numerical Simulation of Pulse Wave Propagation 809
M. Pieniak, K. Cieślicki

Patient Activity Measurement in Active Elbow Orthosis 817
T. Ripel, J. Krejsa, J. Hrbáček

A Physical Model of the Human Circulatory System for the Modeling, Control and Diagnostic of Cardiac Support Processes 825
A. Siewnicka, K. Janiszowski, M. Gawlikowski

A New Method for Tissue Impedance Spectrometry and Its Initial Application *in vivo* 833
M. Władziński, K. Wildner, S. Cygan, B. Grobelski, D. Pawełczak, T. Pałko

Active Artificial Lower Limb 839
M. Zawiski, R. Paśniczek

Evaluation and Testing of Novel Ocular Tactile Tonometry Device 847
E.T. Enikov, P.P. Polyvás, R. Jančo, M. Madarász

Calculation of the Bio-ceramic Material Parameters 855
V. Fuis, P. Janicek

Effect of Contact Condition on Film Thickness Formation in Artificial Joints 863
T. Návrat, M. Vrbka, J. Laštůvka, I. Křupka, M. Hartl, J. Gallo

Mechatronic Education

Model Based Design of a Self-balancing Vehicle: A Mechatronic System Design Case Study 869
R. Grepl

The Design and Use of 3DOF Manipulator as a Platform for Education in Mechatronics 877
D. Klimes, T. Ripel, M. Suransky, J. Vejlupek

Jasper – A Platform for Teaching Mechatronics 883
G. Gaspar, S. Pavlikova, P. Fabo, P. Pavlík

Model-Based Design of Mobile Platform with Integrated Actuator – Design with Respect to Mechatronic Education 891
O. Andrs, Z. Hadas, J. Kovar, J. Vetiška, V. Singule

Author Index 899

Monitoring of Energy Flows in the Production Machines

J. Augste[1], M. Holub[1], R. Knoflíček[1], T. Novotný[1], and J. Vyroubal[2]

[1] Brno University of Technology, Faculty of Mechanical Engineering, Technická 2, 616 69, Brno, Czech Republic
y101686@stud.fme.vutbr.cz

[2] Research Center of Manufacturing Technology, Faculty of Mechanical Engineering, The Czech Technical University in Prague, Horská 3, 128 00, Prague, Czech Republic
J.Vyroubal@rcmt.cvut.cz

Abstract. The article deals with the development of software tools supporting visualization in order to assess the workload of electrical appliances installed in machine-tools. This enables us a considerably easier orientation and the control of energy consumption. The first part of the article is concerned with the application created for simulation of energy flows in the machine-tool with the help of advanced post-processing. That allows software to select to review only interesting data using peaks identifying algorithm. The second part deals with Sankey diagrams visualizations improvements. The tool developed for visualization was applied to the machine FUEQ 125 Efektiv company TOS Kuřim in cooperation with the Czech Technical University in Prague, Faculty of Mechanical Engineering, VCSVTT - Research Centre for Manufacturing Engineering and Technology.

1 Introduction

Energy reduction strategies are increasingly important with the constant increase in electricity costs and the rising environmental awareness of both manufacturers and customers [3]. A machine tool's replacement cycle, after installation, is up to 15–20 years; thus, it is critical to conserve energy on machines with methods that can be applied to both new and existing machines [10]. According to the publication of the European Union, "Ecodesign" aims at improving the environmental performance of products throughout their life-cycle (production, use, and end-of-life) by systematic integration of environmental aspects at the earliest stage of the product design. It is estimated that over 80% of all product related environmental impacts are determined during the design phase, and most of the costs involved are committed then. [11].

This description is very general; therefore, several analyses have to be used for evaluation. The method of "Lowest Life Cycle Cost" (LLCC) allows determining a total cost of ownership and operation of a particular product. LLCC is used to set a particular target minimum of these costs where the space between this minimum

T. Březina and R. Jabłoński (eds.), *Mechatronics 2013*,
DOI: 10.1007/978-3-319-02294-9_1,

and the current state enables us to maintain a space for innovation (competition). To ensure the necessary innovation, the product is compared with the "Best Available Technologies" (BAT); in simple terms, using the best available technologies. These are technologies expected to be introduced into a standard product within a short time horizon. A comparison with the best non-available technologies (BNAT), i.e. with a top of the current state of the art in research and product development, indicates a possible market development in a longer time horizon.

Nevertheless, these analyzing tools are used only to determine the potential for improvement and the direction in which this improvement could occur. The energy-efficiency has to be evaluated [5] for a clear illustration of dependences of the individual variables. Due to complexity of energy flows in productions machines, it is convenient to use a graphical evaluation. That has to summarize data from all the energy-using components. Important points based on peaks and important intervals, for example coolant running, must be identified. Even on a single actuator it is a difficult task because these points could not be easily found without inspection of a smaller interval (Fig. 1).

Therefore, the essence of the proposal is to present improved visual decision-making platform for Ecodesign of machine tool previously described as ECO Design v1.0 [1].

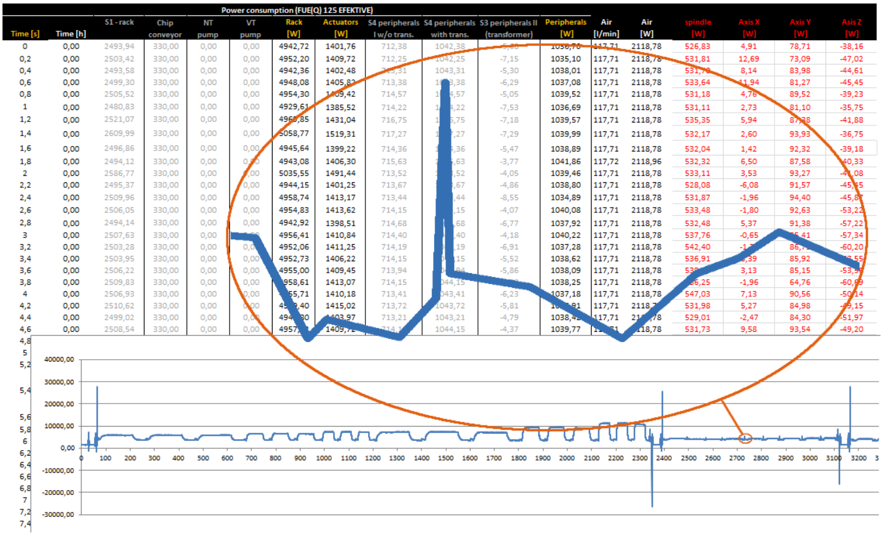

Fig. 1 Example of FU EFEKTIV measured data

2 State of Art

The application must allow a complete support for a product development with regard to energy efficiency [6]. For ECO Design v1.0 application testing data measured (Fig. 1) on floor type machining centre FU EFEKTIV (Fig. 2) were used. Machine FUE (Q) 125 EFEKTIV is installed in TOS Kuřim. Based on testing results some of improvements were suggested by users.

The application itself enables making a straight and comfortable 3D visualization by Sankey diagrams [7] (Fig. 4) but in some cases 2D visualization with a precise value displayed could be more straightforward.

Because the data set sampling time is usually very short, little oscillation of Sankey represented by 3D body could occur. First version of application had implemented frame skip function to make visualizations smoother. Due to 2D diagrams and precise value support request it was necessary to choose different approach to suppress the phenomenon.

Fig. 2 Installed machine FUE(Q) 125 EFEKTIV in TOS Kuřim

3 Peak Analysis

One of typical step towards reducing energy consumption in machine tools is to analyze measured data over all actuators and find peaks and other critical time intervals.

There are several scenarios that have to be reviewed [8]:

- Reduce total energy use for the machine tool based on the usage during idle and non-value-added periods
- Identify disruptions in smooth part production based on anomalous power usage spikes
- Track maintenance state of the machine tool using historical power usage profiles
- Enable environmental reporting on a per-part basis by accurately accounting for the energy use of the part as it is being manufactured

– Notice emerging trends in the energy usage, such as increased total consumption for successive parts which may indicate process plan deviations and inconsistencies.

For peak analysis "window" approach is used. The input is a table of values equally spaced in time. Value in point *i* is local maximum on interval *k* when value of peak function *S* (1) there is bigger than a threshold. The threshold is calculated and a value bigger than zero is adaptively set on dataset. The value is written to matrix *p(i)* for next processing.

$$S(k,i,x_i,T)=\frac{\max\{x_i-x_{i-1},x_i-x_{i-2},\ldots,x_i-x_{i-k}\}+\max\{x_i-x_{i+1},x_i-x_{i+2},\ldots,x_i-x_{i+k}\}}{2} \quad (1)$$

After that local peaks are processed and compared in global context of data set. Point *i* could be global maximum *P(i)* for mean *m'*, standard deviation *s'* and constant *h*.

$$(a[i]-m')>(h*s') \quad (2)$$

Where constant *h* is:

$$1\leq h\leq 3 \quad (3)$$

Peaks close to each other must be removed. Every pair *(i, j)* is tested whenever they are closer than *k* on timeline. When this is true, then just one with larger value is a global maximum.

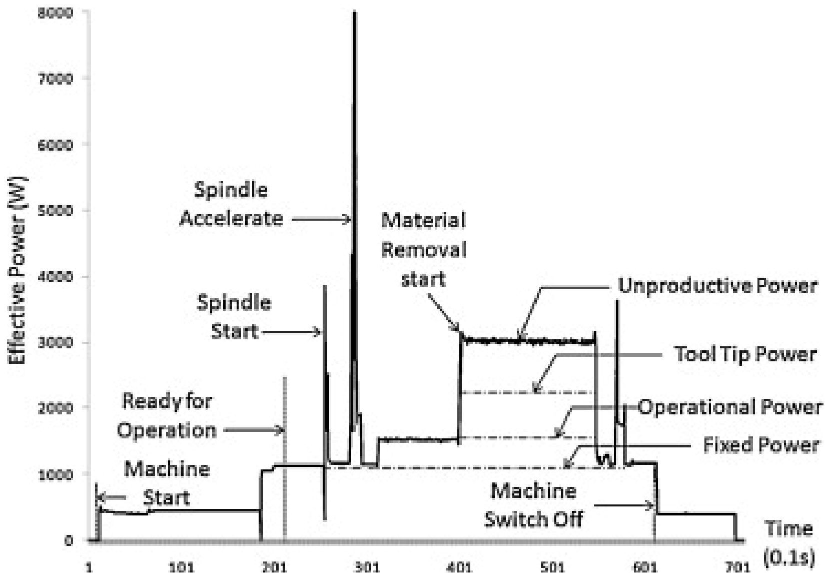

Fig. 3 Visualization of energy flows according to real measured data [2]

4 Sankey Diagrams

They are not visualized together with machine so it could by sometimes hard to understand them. We could also make them as a layer on picture of the machine but machines are usually too complex in the space to show just 2D picture and 3D modeling has been increasingly used for design. Making visualization in 3D enables to obtain a space for extension allowing an increase in the overall visual impression; e.g. by a complex kinematic simulation along with the simulation of energy flows.

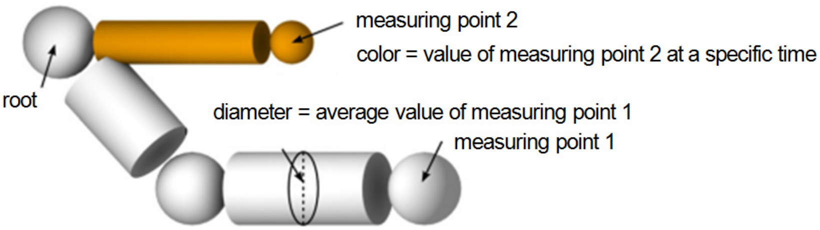

Fig. 4 Example of basic 3D Sankey diagrams [4]

4.1 2D Sankey Diagrams

Suitable design of 2D Sankey diagram for Ecodesign usage was publicized before [9]. It must involve a precise text value to allow users to read accurate value whenever it is needed. Diagrams are showed in separated window (Fig. 5) and were programmed in C# using OpenGL library as well as whole ECO Design application.

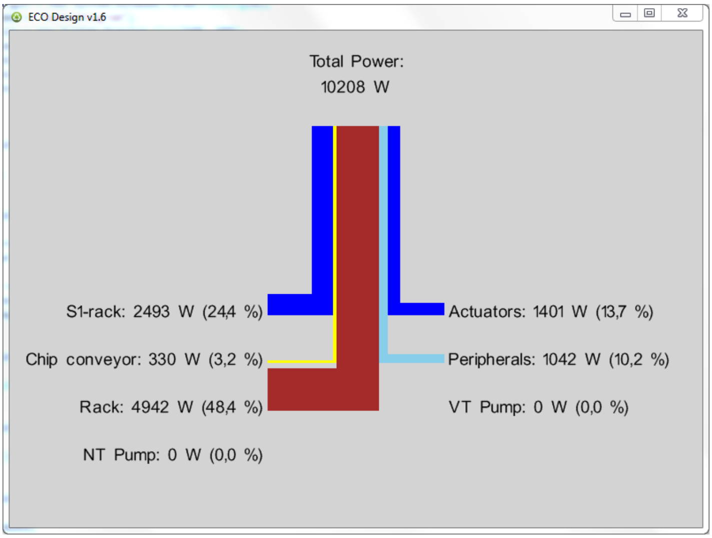

Fig. 5 2D Sankey diagram values according to measured data on FUE(Q) 125

4.2 3D Visualization

During practice testing used source style of 3D Sankey (Fig. 4) visualization was a little bit modified. Different visualization approach (Fig. 6) was designed to get better information value into visualization. There is a static basic color used for identification of object, combination of intensity of each color for indication of growth, transparency for average value and diameter for actual value. Indication of growth helps to predict peak states (Chapter 3) before they occur. Using transparency to visualize average value helps to highlight parts with significant energy consumptions compared to the other ones.

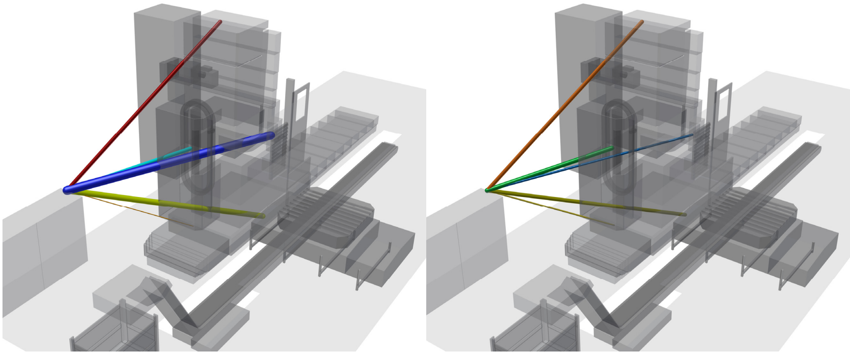

Fig. 6 Visualization of energy flows; values represented by diameter of bodies

5 Conclusions

The Eco Design v1.6 has been designed to provide energy flows post-processing to production machines designers. One of typical tasks realized in software is to analyze measured data over all actuators and find peaks and other critical time intervals. The main target is to find the peaks creation process. Thanks to implementation of 3D visualization, possible improvements of process could be suggested. On the other hand, 2D Sankey diagram enables precise value checking and, therefore adds the possibility to select from several variants. All of these functions and possibilities form a visual decision-making platform for Ecodesign.

Main possible future developments of the software are connections to virtual reality and augmented reality visualizations. Data review in CAVE using virtual reality for presentation of final results could show different states even on very complex machines and complexly solve Ecodesign study together with all other studies necessary to be done in design phase. On the other hand, augmented reality enables to changes overall impact to energy flows and consumption of the production machine.

Acknowledgments. This work has been supported by Brno University of Technology, Faculty of Mechanical Engineering, Czech Republic (Grant No. FSI-S-11-5). This project has been funded with support from the state budget through the Ministry of Industry and Trade of the Czech Republic (ID of project: FR-TI3/655 – ECODESIGN in tool machine construction) and by European Regional Development Fund in the framework of the research project NETME Centre under the Operational Programme Research and Development for Innovation. Reg. Nr. CZ.1.05/2.1.00/01.0002, id code: ED0002/01/01, project name: NETME Centre – New Technologies for Mechanical Engineering.

References

[1] Augste, J., Knoflíček, R., Holub, M., Novotný, T.: Tools for visualization of energy flows in the construction of machine- tools. MM Science Journal, 392–395 (March 2013) ISSN: 1803- 1269

[2] Duflou, J.R., et al.: Towards energy and resource efficient manufacturing: A processes and systems approach. CIRP Annals - Manufacturing Technology 61(2), 587–609 (2012) ISSN 0007-8506

[3] Behrendt, T., et al.: Development of an energy consumption monitoring procedure for machine tools. CIRP Annals - Manufacturing Technology 61(1), 43–46 (2012) ISSN 0007-8506

[4] Neugebauer, R., et al.: VR tools for the development of energy-efficient products. CIRP Journal of Manufacturing Science and Technology 4(2), 208–215 (2011) ISSN 1755-5817

[5] Götze, U., et al.: Integrated methodology for the evaluation of the energy- and cost-effectiveness of machine tools. CIRP Journal of Manufacturing Science and Technology 5(3), 151–163 (2012) ISSN 1755-5817

[6] Rünger, G., et al.: Development of energy-efficient products: Models, methods and IT support. CIRP Journal of Manufacturing Science and Technology 4(2), 216–224 (2011) ISSN 1755-5817

[7] Sankey, H.R.: The Thermal Efficiency of Steam-Engines. MPICE 134, 278–283 (1898)

[8] Vijayaraghavan, A., Dornfeld, D.: Automated energy monitoring of machine tools. CIRP Annals - Manufacturing Technology 59(1), 21–24 (2010) ISSN 0007-8506

[9] Behrendt, T., Zein, A., Min, S.: Development of an energy consumption monitoring procedure for machine tools. CIRP Annals - Manufacturing Technology 61(1), 43–46 (2012) ISSN 0007-8506

[10] Oda, Y., et al.: Study of optimal cutting condition for energy efficiency improvement in ball end milling with tool-workpiece inclination. CIRP Annals - Manufacturing Technology 61(1), 119–122 (2012) ISSN 0007-8506

[11] European Union. (2008) Draft Working Plan of the Ecodesign Directive (2009–2011), `http://www.eup-network.de/fileadmin/user_upload/Produktgruppen/Arbeitsplan/DraftWorkingPlan_28Apr08.pdf`

Off- Road Vehicle with Controlled Suspension in Soft Unprepared Terrain

A. Bílkovský[1] and Z. Šika[2]

[1] VUTS, a. s., Svarovska 619, 460 01, Liberec XI, Czech Republic
ales.bilkovsky@vuts.cz
[2] Czech Technical University in Prague, Faculty of Mechanical Engineering, Department of Mechanics, Biomechanics and Mechatronics, Technicka 4, 166 07, Praha, Czech Republic
zbynek.sika@fs.cvut.cz

Abstract. The paper deals with the investigation of the influence of the controlled suspension on the traction capability of the off-road vehicles, especially the agriculture tractors. The standard suspension of the tractor is realized by tires, the rear axle is firm. The controlled suspension is used to increase traction forces in the soft unprepared terrain. The models of wheel soil interaction describe the rigid and elastic models of wheel based on semi-empirical model.

1 Introduction

The prediction of the tractive and traction force is very important but it is very difficult. It depends on correct of models of terrain, the correct parameters of terrain and on model of the tire. The agricultural off-road vehicles are built with firm rear axle and the suspension of this vehicle is realized by tires. The suitable controlled suspension influences the motion of the vehicle in the terrain and the forces between the terrain and the wheel.

2 Modeling Elements

The basic model's elements for modeling of the vehicle in the terrain were used. The model describes the basic characteristic response of the real object. The model is consists of the vehicle model, the terrain and soil model and the wheel-soil interaction model. Each of models will be described below.

2.1 Vehicle Model

A 4-DOF half vehicle model is implemented to simulate the response of vehicle on different loading, terrain profile and to calculate the load on wheels.

T. Březina and R. Jabłoński (eds.), *Mechatronics 2013*,
DOI: 10.1007/978-3-319-02294-9_2,

The four degrees of freedom of the vehicle are the heave, pitch and bounces of the two unsprung masses. The vehicle model (Fig. 1) is half car model and consists of body (sprung mass), two suspension systems and two wheels. Each of suspension system consists of linear spring and damper. The wheel is modeled as a linear spring too. The front suspension has stiffness k_f and damping b_f, the rear suspension has stiffness k_r and damping b_r.

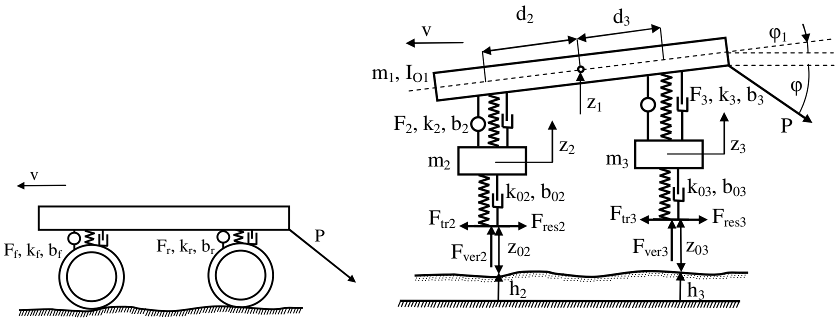

Fig. 1 Half car model

The set of ODE of vehicle model motion is obtained by Newton's method [6] as follows

$$\begin{aligned} m_1\ddot{z}_1 = &-k_2(z_1 - d_2\varphi_1 - z_2) - b_2(\dot{z}_1 - d_2\dot{\varphi}_1 - \dot{z}_2) - \\ &- k_3(z_1 + d_3\varphi_1 - z_3) - b_3(\dot{z}_1 - d_3\dot{\varphi}_1 - \dot{z}_3) - m_1 g - P\cos\varphi \end{aligned} \quad (1)$$

$$\begin{aligned} I_{01}\varphi_1 = &\, k_2(z_1 - d_2\varphi_1 - z_2)d_2 - b_2(\dot{z}_1 - d_2\dot{\varphi}_1 - \dot{z}_2)d_2 - \\ &- k_3(z_1 + d_3\varphi_1 - z_3)d_3 - b_3(\dot{z}_1 - d_3\dot{\varphi}_1 - \dot{z}_3)d_3 - M_P \end{aligned} \quad (2)$$

$$m_2\ddot{z}_2 = k_2(z_1 - d_2\varphi_1 - z_2) + b_2(\dot{z}_1 - d_2\dot{\varphi}_1 - \dot{z}_2) - m_2 g - F_{ver2} \quad (3)$$

$$m_3\ddot{z}_3 = k_3(z_1 + d_3\varphi_1 - z_3) + b_3(\dot{z}_1 + d_3\dot{\varphi}_1 - \dot{z}_3) - m_3 g - F_{ver3} \quad (4)$$

2.2 *Terrain and Soil Model*

In this study we used one type terrain profile to simulate the dynamic response of vehicle, illustrated in Fig. 2. The combination of loading of a pulled object and the terrain prepare the simulation conditions.

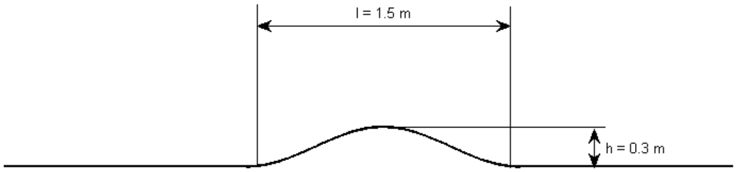

Fig. 2 Terrain profile

The mobility of wheel vehicle on soft terrain is determined by pressure sinkage relation and shear stress – shear displacement relation, which are established at the contact patch between the tire and the soil.

Typical parameters of the terrain are measured by the experimental method. The empirical and semi-empirical approaches is used to describe these relations as [1],[2] and [3]. The terrain is characterized by parameters, which are in Tab. 1. There are presented parameters for several types of the terrain.

Table 1 Parameters of terrains – taken from [2]

Terrain	n -	k_c (kN/m^{n+1})	k_ϕ (kN/m^{n+2})	c (kN/m^2)	ϕ (°)	K (m)
Grenville Loam	1.02	66.0	4486	3.1	29.8	0.038
Upland Sandy Loam (type 1)	1.1	74.6	2080	3.3	33.7	0.093
Upland Sandy Loam (type 2)	0.85	3.3	2529	2.5	28.2	0.041
Upland Sandy Loam (type 3)	1.74	259	1643	3.3	33.7	0.093

The most commonly used relations in terramechanics are Bekker's equation for pressure sinkage relation, shown in Eq. (5) and Janosi-Hanamoto equation for shear stress – shear displacement relation shown in Eq. (6).

$$p=\left(\frac{k_c}{b}+k_\phi\right)z^n \tag{5}$$

$$\tau=[c+p\tan\varphi]\ (1-e^{(-j/K)}) \tag{6}$$

3 Models of Wheel

The wheel of the off-road vehicle is modeled as a rigid or an elastic wheel. It depends on critical pressure, which is compared with the average ground pressure. When the critical pressure is less than the average ground pressure, the tire is modeled as rigid. The average ground pressure is sum of tire inflation pressure and the terrain pressure due to carcass stiffness [1].

In other comparison of the rigid and the elastic wheel the depth of sinkage is used. When the depth of sinkage of rigid wheel and the depth of sinkage of elastic wheel are computed, these values are compared. When the sinkage of rigid wheel is higher then sinkage of elastic wheel, the wheel is modeled as the elastic. Otherwise, the wheel is modeled as rigid wheel.

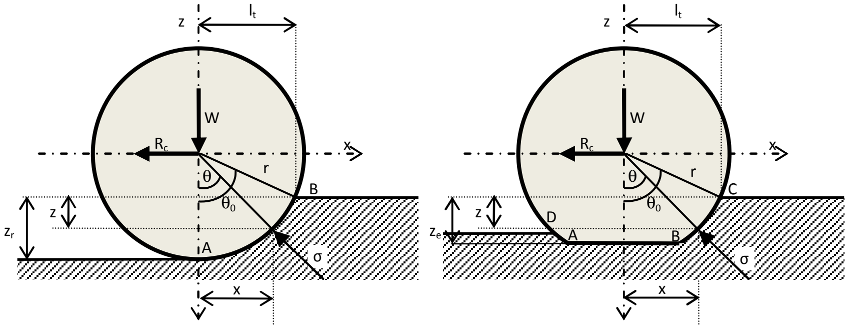

Fig. 3 Rigid and elastic model of the wheel

3.1 Rigid Wheel

When the wheel is modeled as rigid, the deformation of the terrain occurs. The wheel is not deformed. For the tire model, the sinkage is calculated by Eq. (7) and the shear displacement is calculated by Eq. (9) [2], [4].

$$z_r = r(1-\cos\theta_0) = \left[\frac{3W}{b(3-n)(k_c/b+k_\phi)\sqrt{2r}}\right]^{\frac{2}{2n+1}} \tag{7}$$

$$z_\theta = r\cos\theta - r + z_r \tag{8}$$

$$j = r[(\theta_0-\theta)-(1-i)(\sin\theta_0-\sin\theta)] \tag{9}$$

Substituting Eq. (5), Eq. (6) and Eq. (9) into the tractive force F (Eq.(10)), resistance force Rc (Eq.(11)) and drawbar pull force Fd (Eq.(12)) are calculated.

$$F = \int_0^{\theta_0} \tau(\theta)\cos\theta\cdot r\cdot b\cdot \mathrm{d}\theta \tag{10}$$

$$R_c = \int_0^{\theta_0} p(\theta)\sin\theta\cdot r\cdot b\cdot \mathrm{d}\theta \tag{11}$$

$$F_d = F - Rc \tag{12}$$

3.2 Flexible (elastic) Wheel

The elastic wheel model is used in case of deformation of the tire and the terrain. The circumference is divided into three parts as shown in Fig.3: input part BC, flat part AB and part or relaxing AD.

For the first section BC, the maximum sinkage and sinkage at any angle are Eq. (13) and Eq. (14).

$$z_e = \left(\frac{p_{agr}}{k_c / b + k_\phi} \right)^{1/n} \tag{13}$$

$$z_{BC} = r(\cos\theta - \cos\theta_0) \tag{14}$$

The shear displacement *j* developed along section BC can be determined in the same way as that earlier described for the rigid wheel [1], [2]. For the section AB the slip velocity is constant. The increase in shear displacement along section AB is proportional to the slip of tire and distance x between the points AB. The shear displacement along the section AD can be determined by the same way as that discussed previously.

4 Controlled Suspensions

The controlled suspension using in the model is based on Extended Ground Hook, called as “Skyhook”. In Fig. 4 there is the representation of the theoretical approach and the realizing by the control law. This control is used with controllable damper. The characteristic of the controlled damper is shown in Fig. 4.

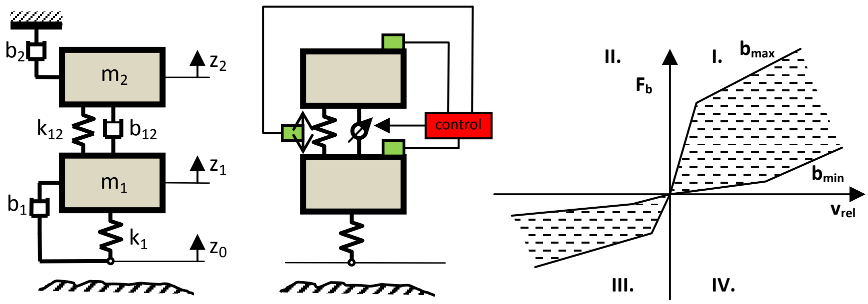

Fig. 4 Extended Ground Hook – theoretical, realization, characteristic of controlled damper

The control law [5] (Eq.(15)) is based on selection of parameters according to relative velocity between sprung and unsprung masses – as shown in Fig. 4.

$$F_b = b_{12}\,(\dot{z}_2 - \dot{z}_1) + b_2\,\dot{z}_2 - b_1(\dot{z}_1 - \dot{z}_0 + \dot{h}) \qquad (15)$$

5 Numerical Results

To analyze of response of 4-DOF vehicle with the wheel – soil interaction the model runs the straight forward driving on Grenville loam. The vehicle runs over the hump (Fig. 2). The multi object parameter optimization of the controlled suspension was used. The optimized parameters were obtained. The next simulations were computed for obtained parameters for controlled suspension and then the results of response were compared with the vehicle with firm rear axle (usprung model) and with the rear suspension model (sprung model).

The vehicle runs straight forward with constant velocity 10 m/s, but real velocity of vehicle is lower, because during the running over the hump the slip increases. The wheel rotates with the constant velocity, but the vehicle is running slower (Fig. 5).

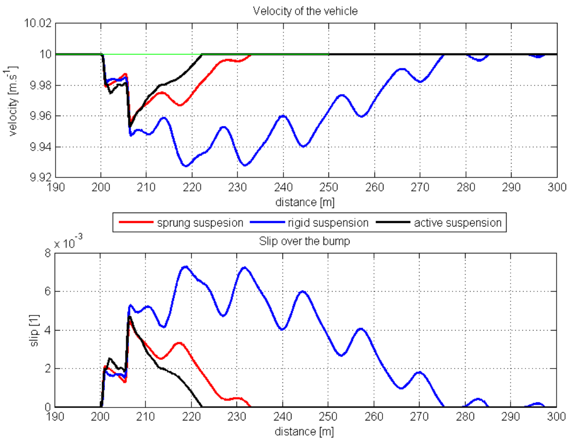

Fig. 5 Velocity of the vehicle running over the hump

The effect of the suspension and the tire stiffness uncertainty on the vehicle performance is shown in Fig 6. The heave of chassis is for unsprung model very uncomfortable, but for controlled suspension the heave is more comfortable. If the firm axle is used, the vehicle is not so inclined, but if the sprung axle is used, the vehicle is more inclined. This is results of sprung suspension; the construction changes can eliminate this fact.

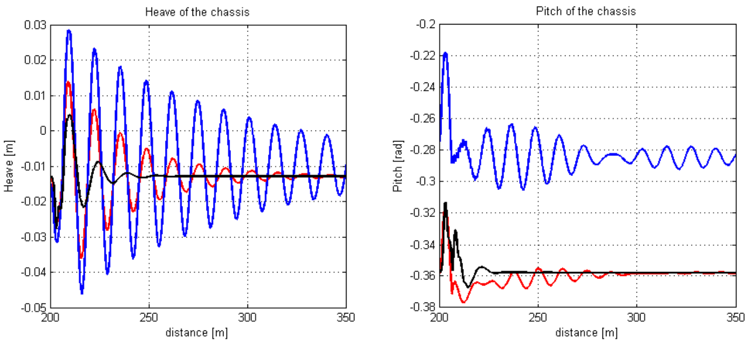

Fig. 6 Heave and pitch of the chassis

The effect of the suspension on the wheel – soil interaction forces is considerable. The tractive force and resistance force depend on soil parameters, on the geometry of the tire and on the vertical force operation on the wheel. The sinkage of the wheel increase, if the vertical force increases too. The resistance force depends on the sinkage and the force increase with the sinkage together. The results of tractive force minus resistance forces (depend on models, but buldozering effect, the deformation of tire are examples of resistance force) is drawbar pull (Fig. 7). This force represents the free capacity of wheel – soil interaction.

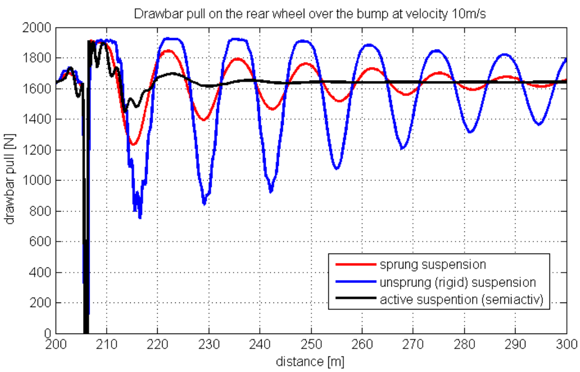

Fig. 7 Drawbar pull on the rear wheel over the hump at velocity 10m/s

6 Conclusions

This paper presents the influence of controlled suspension on the vehicle in the terrain. This is a way how to study the wheel – soil interaction and compare several models of vehicles. The prediction of mobility and performance of the off-road vehicle depend on realistic parameters, but the response of the simulation vehicle is similar. The results of simulation confirm that the controlled suspension increases the drawbar pull and enhances the comfort for the driver. The increase of mobility of the vehicle depends on the controlled suspension.

References

[1] Wong, J.Y.: Theory of Groung Vehicles. John Wiley, New York (2001)

[2] Wong, J.Y.: Terramechanics and Off-Road Vehicles. Elsevier Science Publisher, Amsterdam (1989)

[3] Muro, T., O'Brien, J.: Terramechanics: land locomotion mechanics. A.A. Balkema Publishers, Exton (2004)

[4] Li, L., Sandu, C.: On the impact of cargo weight, vehicle parameters, and terrain characteristics on the prediction of traction for off-road vehicles. Journal of Terramechanics 44(3), 221–238 (2007)

[5] Valášek, M., Novák, M., Šika, Z., Vaculín, O.: Extended Ground-Hook - New Concept of Semi-Active Control of Truck's Suspension. Vehicle System Dynamics 27(5-6), 289–303 (1997)

[6] Stejskal, V., Valášek, M.: Kinematics and dynamics of machinery. Marcel Dekker, New York (1996)